# Structure−Activity Relationships of Cyanoquinolines with Corrector−Potentiator Activity in ΔF508 Cystic Fibrosis Transmembrane Conductance Regulator Protein

John M. Knapp,[†] Alex B. Wood,[†] Puay-Wah Phuan,[‡] Michael W. Lodewyk,[†] Dean J. Tantillo,[†] A. S. Verkman,[‡] and Mark J. Kurth*[,†]

[†]Department of Chemistry, University of California, Davis, California 95616, United States

[‡]Departments of Medicine and Physiology, University of California, San Francisco, California 94143-0521, United States

Ⓢ Supporting Information

ABSTRACT: Cystic fibrosis (CF) is caused by mutations in the cystic fibrosis transmembrane conductance regulator (CFTR) chloride channel. The most common CF-causing mutation, ΔF508-CFTR, produces CFTR loss-of-function by impairing its cellular targeting to the plasma membrane and its chloride channel gating. We recently identified cyanoquinolines with both corrector ("Co", normalizing ΔF508-CFTR targeting) and potentiator ("Po", normalizing ΔF508-CFTR channel gating) activities. Here, we synthesized and characterized 24 targeted cyanoquinoline analogues to elucidate the conformational requirements for corrector and potentiator activities. Compounds with potentiator-only, corrector-only, and dual potentiator−corrector activities were found. Molecular modeling studies (conformational search ⇒ force-field lowest energy assessment ⇒ geometry optimization) suggest that (1) a flexible tether and (2) a relatively short bridge between the cyanoquinoline and arylamide moieties are important cyanoquinoline-based CoPo features. Further, these CoPo's may adopt two distinct π-stacking conformations to elicit corrector and potentiator activities.
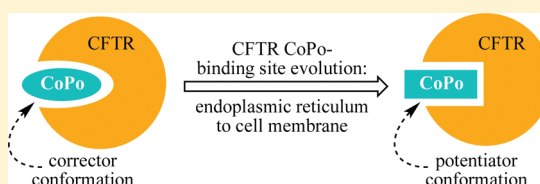
INTRODUCTION

Cystic Fibrosis (CF) is a genetic disorder caused by mutations in the cystic fibrosis transmembrane conductance regulator (CFTR) protein,[1] which is expressed in epithelia in lung, pancreas, intestine, testis, and other tissues.[2] While there are many CF-causing mutations, the most common CFTR mutation is a deletion of the phenylalanine residue at position 508 (ΔF508-CFTR). The ΔF508 mutation causes folding and conformation defects resulting in its retention in the endoplasmic reticulum and accelerated degradation.[3,4] Additionally, any ΔF508-CFTR that reaches the cell plasma membrane is poorly functional as a chloride channel.[2] Consequently, the ΔF508-CFTR mutation results in greatly reduced cell membrane chloride permeability.

An ideal small molecule treatment of CF would fully restore ΔF508-CFTR structure to the native wild type state, resulting in normalization of its cellular processing and chloride channel function.[5] Such compounds have not been identified. Instead, separate compounds, called "correctors", which partially rescue ΔF508-CFTR cellular misprocessing, and "potentiators", which partially restore ΔF508-CFTR chloride channel function, have been identified (Figure 1). We and others have identified a variety of correctors[6] (e.g., **1** {N-(2-((5-chloro-2-methoxyphenyl)amino)-4′-methyl-[4,5′-bithiazol]-2′-yl)-benzamide, corr-4a}[6d] and **2** {4-(cyclohexyloxy)-2-(1-(4-((4-methoxyphenyl)sulfonyl)piperazin-1-yl)ethyl)quinazoline, VRT-325};[6h] Figure 1a) and potentiators[7] (e.g., **3** {2-(2-(1H-indol-3-yl)-N-methylacetamido)-N-(4-isopropylphenyl)-2-phe-

nylacetamide, PG01}[7g] and **4** {N-(2,4-di-tert-butyl-5-hydrox-yphenyl)-4-oxo-1,4-dihydroquinoline-3-carboxamide, VX-770};[7h] Figure 1b). Recently, we identified a dual-acting cyanoquinoline having independent corrector and potentiator activities (**5**, {N-(2-((3-cyano-5,7-dimethylquinolin-2-yl)-amino)ethyl)-3-methoxybenzamide, CoPo-22};[8] Figure 1c). Such compounds would be advantageous over CF treatments requiring separate corrector and potentiator administration.[8] Moreover, the development costs for a single drug that treats both defects would be significantly lower than development costs for a two-drug paradigm.

Cyanoquinoline **5** contains three distinct subunits consisting of a cyanoquinoline core and arylamide moieties linked by a flexible tether (Figure 1). We postulated that this tether allows **5** to adopt two active conformations, an active corrector conformation and an active potentiator conformation, and that altering this tether would modulate CoPo activities by restricting its conformations. The two active conformations of **5** could allow binding to two separate targets (mode 1), two distinct binding sites on the same target (mode 2), or two different forms of a single binding site on ΔF508-CFTR that change shape during protein transport from the endoplasmic reticulum (ER) to the cell plasma membrane (mode 3, Figure 2). Of these, mode 3 appears to be the most likely on a statistical basis; i.e., one molecule addressing one binding site
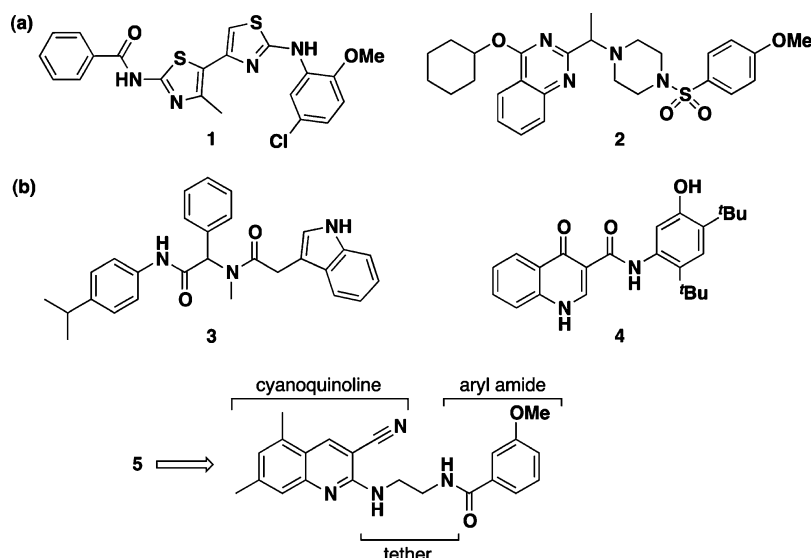
Figure 1. Structures of (a) correctors **1** and **2**, (b) potentiators **3** and **4**, and (c) cyanoquinoline **5** with structural subunits identified.

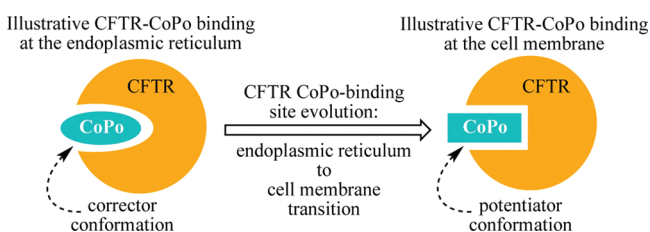**Figure 2.** Possible CoPo conformational adaptation during the ER ⇒ cell membrane transition.

that changes shape as it matures is statistically less challenging than one molecule addressing two distinct binding sites (modes 1 and 2). The goal of the work reported here was to examine how the tethering moiety in **5** influences its ability to afford both corrector (Co) *and* potentiator (Po) activities and to assess the feasibility of mode 3 by computational analysis of the proclivities of **5** and tethered analogues for particular conformations.

■ CHEMISTRY

This study examines the role of the tether and, secondarily, the arylamide subunits on CoPo activities. Our tether-focused strategy is depicted in Figure 3 where the cyanoquinoline
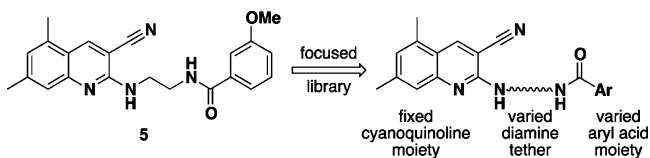

Figure 3. Tether-focused CoPo library diversification strategy.

moiety is fixed while the tether and arylamide moieties are varied. Indeed, quinolines hold privileged heterocycle status[9] and have received much attention as antibacterial agents[10] and cancer therapeutics.[11] Their biological importance has led to the development of several strategies to construct this aromatic ring system.

The CoPo cyanoquinoline core was synthesized starting from commercially available 3,5-dimethylaniline **6** (Scheme 1).

**Scheme 1. Synthesis of Chlorocyanoquinoline Intermediate 5**[a]
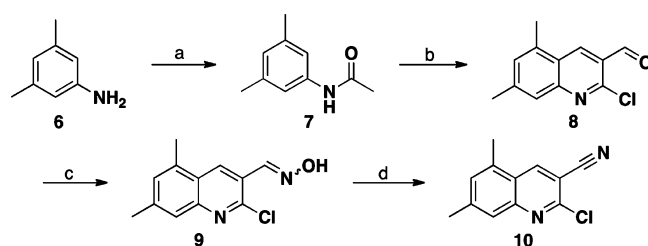
[a]Reagents: (a) acetic anhydride, THF; (b) POCl₃, DMF; (c) NH₂OH·HCl, Et₃N, EtOH; (d) SOCl₂, benzene.

Acylation of **6** with acetic anhydride gave **7** in near quantitative yield, and subsequent Vilsmeier−Haack[12] type reaction gave chloroquinoline carboxaldehyde **8**. Neutralization, filtration, and drying produced pure **8** in 95% yield. Aldehyde **8** was then condensed with hydroxylamine to yield oxime **9**, which was directly converted to nitrile **10** by dehydration with SOCl₂ in refluxing benzene (93% yield over two steps).

Aromatic substitution of **10** with various diamines allowed for ready diversification of the tethering subunit as depicted in Scheme 2. The tethers examined were derived from 1,2-diaminoethane (the tether in original screening hit **5**), 1,3-

Scheme 2. Tether Diversification[a]
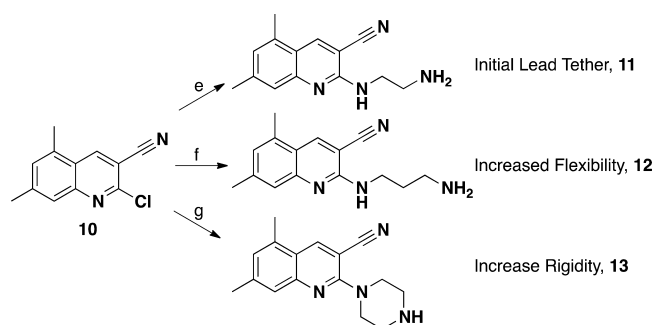
[a]Reagents: (e) 1,2-diaminoethylene, dioxane, reflux; (f) 1,3-diaminopropylene, dioxane, reflux; (g) piperazine, dioxane, reflux.
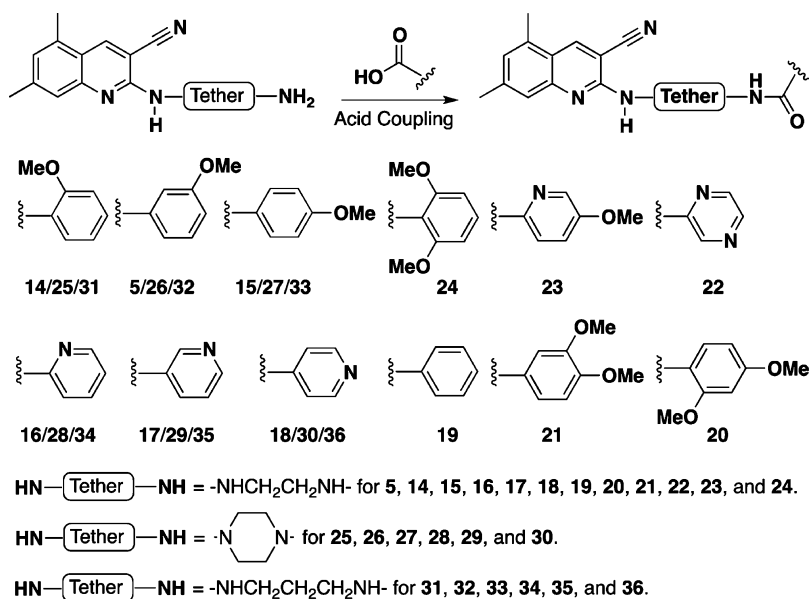
Figure 4. Cyanoquinoline-based CoPo arylamide diversity.

diaminopropane (a longer and more flexible tether), and 1,4-piperazine (a more rigid tether). All three diamino tethers gave their intended products (**10 → 11−13**) in good yields (61−62%).

Further diversification of the distal primary or secondary amine in **11−13** was accomplished by EDC-mediated aryl acid coupling (Figure 4). Heteroaromatic amides were not evaluated in our initial screening study. So, as a preliminary test of the effect of heterocycles on CoPo potency, a range of pyridyl acids, an array of arylmethoxy acids (similar to that of initial hit **5**), and one methoxypyridyl acid were employed in the acylation of **11−13**. The specific aryl acids used in this coupling step are depicted in Figure 4.

■ PHARMACOLOGY

ΔF508-CFTR correctors were previously identified by screening of a large collection of diverse small molecules.[6d] Our screening assay utilized Fischer rat thyroid (FRT) epithelial cells coexpressing ΔF508-CFTR and the yellow fluorescent protein (YFP) halide indicator YFP-H148Q/I152L at 37 °C in a 96-well-plate format. Test compounds at 10 μM (and negative/positive controls) were added to each well for 18−24 h. ΔF508-CFTR-facilitated iodide influx was determined from the kinetics of decreasing YFP fluorescence following addition of extracellular iodide in the presence of the potentiators genistein and forskolin. Active compounds from the primary high-throughput screen were verified and then counterscreened for ΔF508-CFTR potentiator activity. For the potentiator assay ΔF508-CFTR was low-temperature rescued by incubating FRT cells coexpressing ΔF508-CFTR and YFP at 27 °C for 24 h. Test compounds at 25 μM (and negative/positive control) were added to each well for 10 min in the presence of forskolin. Similar to the corrector assay, ΔF508-CFTR-facilitated iodide influx was determined from the kinetics of decreasing YFP fluorescence following addition of extracellular iodide.
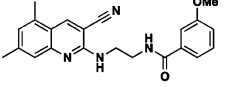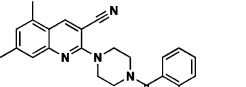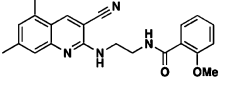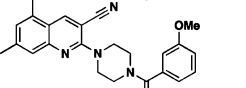
■ COMPUTATIONS
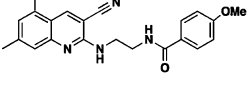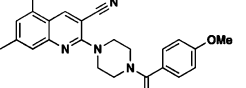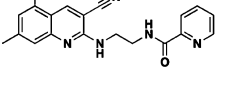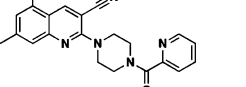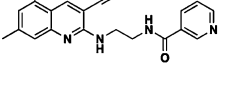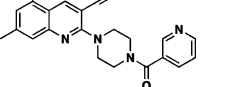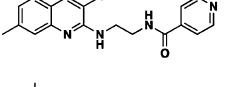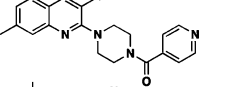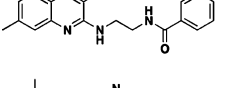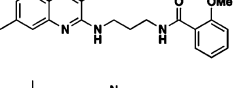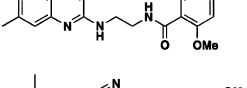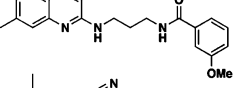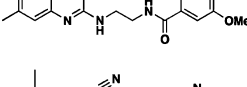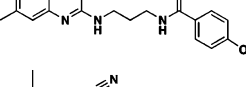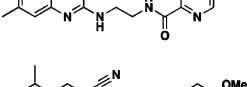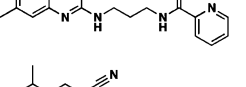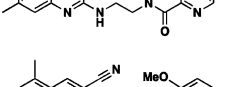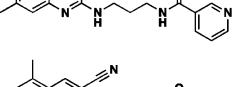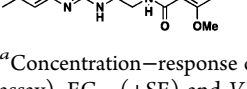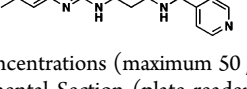
For cyanoquinolines **5** and **26**, a two-step conformational search was performed. First, candidate conformers were identified via a systematic search in Spartan '10[13] in which

each bond between the aryl moieties was given 2-fold rotational freedom (sp²−sp² bonds) or 3-fold rotational freedom (sp²−sp³ and sp³−sp³ bonds) and atoms in rings were given 3-fold puckering mobility. This procedure resulted in 36 candidate conformations for **5** and 42 candidate conformations for **26**, each within 10 kcal/mol of the lowest energy conformation, as assessed by the MMFF94 force field.[14] These candidates were then subjected to further geometry optimization using the M06-2X/6-31+G(d,p)[15] density functional theory method as implemented in the Gaussian '09 software suite.[16] After this refinement, five conformers within 3 kcal/mol of the lowest energy conformer of **5** and 18 conformers within 3 kcal/mol of the lowest energy conformer of **26** (four within 2 kcal/mol) were found, as assessed by computed electronic energies with solvent (water) modeled by the SMD continuum solvation model[17] (via single-point calculations). Finally, select conformers described below were further refined with full solvent optimization and frequency calculations in order to include entropy contributions to the computed relative free energies. Atomic coordinates and computed energies for all structures can be found in the Supporting Information. As described below, constrained calculations were also performed on some conformers.

■ RESULTS AND DISCUSSION

Corrector and potentiator activities for the 24 cyanoquinolines synthesized in this study were assayed separately in ΔF508-CFTR expressing FRT epithelial cells. Table 1 lists corrector (Co) and potentiator (Po) activities as EC_{50} and V_{max} from concentration-dependence studies. EC_{50} is a measure of compound potency and V_{max} is a measure of compound efficacy in increasing cell chloride permeability. Figure 5 shows representative concentration-dependence data for the corrector and potentiator plate reader assays from which EC_{50} and V_{max} values were deduced from concentration-dependence data by nonlinear regression as described in the Experimental Section (plate reader assay). Figure 6 shows representative short-circuit assays of corrector and potentiator activities of compound **15**, compared to **5**, in which apical membrane chloride current was measured in the ΔF508-CFTR expressing FRT cells after

Table 1. Corrector and Potentiator Activities, Determined in Triplicate, of CoPo Analogues As Measured by Fluorescence Plate–Reader Assay[a]

Structure	CoPo	Corrector EC_{50} (μM)	Corrector V_{max} (μM/s)	Potentiator EC_{50} (μM)	Potentiator V_{max} (μM/s)	Structure	CoPo	Corrector EC_{50} (μM)	Corrector V_{max} (μM/s)	Potentiator EC_{50} (μM)	Potentiator V_{max} (μM/s)
	5	2.2 ± 0.3	300	5.9 ± 0.5	216		25	inactive	--	1.0 ± 0.3	129
	14	11.0 ± 0.9	114	2.3 ± 0.4	154		26	inactive	--	1.2 ± 0.3	200
	15	3.0 ± 0.3	172	4.1 ± 1.0	181		27	inactive	--	1.3 ± 0.2	281
	16	inactive	--	1.2 ± 0.4	80		28	inactive	--	7.4 ± 0.3	102
	17	2.7 ± 0.6	151	13.2 ± 0.6	242		29	inactive	--	inactive	--
	18	7.3 ± 0.8	176	10.0 ± 3.1	220		30	inactive	--	inactive	--
	19	inactive	--	10.0 ± 2.0	210		31	inactive	--	27.6 ± 2.0	254
	20	4.2 ± 0.4	108	55.0 ± 3.5	426		32	4.6 ± 0.2	134	4.6 ± 0.4	147
	21	1.5 ± 0.4	380	48.0 ± 5.0	216		33	4.3 ± 0.2	112	5.0 ± 0.2	231
	22	6.7 ± 1.0	174	inactive	--		34	inactive	--	6.1 ± 0.2	233
	23	2.7 ± 0.5	88	3.4 ± 0.5	70		35	3.0 ± 0.5	140	16.0 ± 0.3	115
	24	3.7 ± 0.6	111	11.5 ± 1.0	119		36	8.2 ± 0.4	61	13.2 ± 0.4	53

[a]Concentration–response curves were determined for eight compound concentrations (maximum 50 μM for potentiator assay; 25 μM for corrector assay). EC_{50} (±SE) and V_{max} were computed as described in the Experimental Section (plate reader assay).
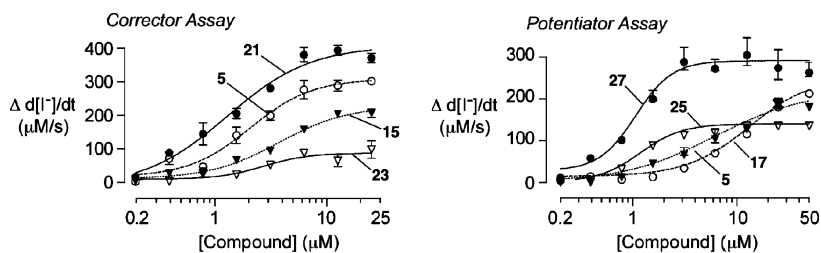

Figure 5. Concentration-dependence of corrector (left) and potentiator (right) activities of indicated compounds in FRT cells expressing ΔF508-CFTR measured by iodide (I^-) influx. See Table 1 for summary of deduced EC_{50} and V_{max}.
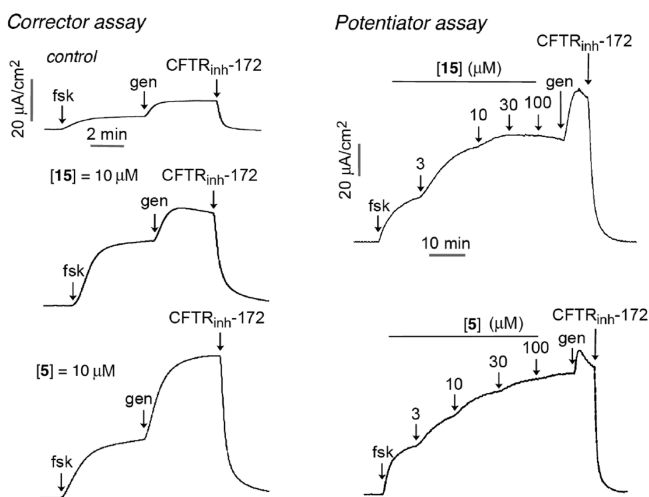
Figure 6. Short-circuit current measurement of ΔF508-CFTR chloride conductance. Measurements of corrector and potentiator activities of **15** and **5** were done in the presence of an apical-to-basolateral chloride gradient in basolateral membrane-permeabilized cells. Added compounds included forskolin (fsk, 20 μM), genistein (gen, 50 μM), and CFTR_inh-172 (10 μM).

basolateral membrane permeabilization and in the presence of a transepithelial chloride gradient. The corrector assay was done by incubation of cells for 18−24 h with test compound at 37 °C, followed by addition of forskolin and the potentiator genistein. The potentiator assay was done in low temperature-rescued cells by addition of forskolin followed by test compound. Short-circuit data as in Figure 6 confirmed the main findings obtained using the fluorescence plate reader assay.

On the basis of these function studies, 12 compounds in this series were identified as having both corrector and potentiator activities (**14**, **15**, **17**, **18**, **20**, **21**, **23**, **24**, **32**, **33**, **35**, and **36**), 8 compounds were identified as having potentiator-only activity (**16**, **19**, **25−28**, **31**, and **34**), and 1 compound was identified as having corrector-only activity (**22**). For compounds having both corrector and potentiator activities, cyanoquinoline **5** is the most active (corrector/potentiator values of 2.2 μM/5.9 μM): the corrector activity EC_{50} values for cyanoquinolines **15**, **17**, and **18** were 3.0, 2.7, and 7.3 μM, respectively, and the potentiator activity EC_{50} values were 4.1, 13, and 10 μM, respectively. The maximal efficacies, V_{max}, of cyanoquinoline **5** for corrector and potentiator actions are comparable with those of **1** and genistein, respectively.

Two notable observations from these data are that constraining the diamino tether in a piperazine ring abolished corrector activity but, conversely, resulted in excellent potentiator activity (**25−27**), better than that of **5**. One interpretation of these findings is that that the binding site evolves during the endoplasmic reticulum ⇒ cell membrane transition (mode 3 discussed above; see Figure 2) and that piperazine-constrained cyanoquinolines cannot adequately adapt to the ΔF508-CFTR corrector-binding site when the protein is in the endoplasmic reticulum. Consequently, transport to the cell membrane does not occur with these piperazine-constrained cyanoquinolines. Conversely, an increase in mobility of the chain by lengthening (ethylene → propylene) results in CoPo's (**32−33**, **35**, **36**) with comparable, albeit, lower corrector and potentiator activity compared to that of **5**. This increased tether chain length causes increased flexibility and different conformational preferences, which in turn results in a reduced probability of these CoPo's adopting an active conformation. Thus, the propylene-based tether is slightly less active compared to the ethylene-based tether.

If this model is correct, then the action of cyanoquinoline-based CoPo's likely involves a slight, but important, conformational change allowing them to adapt to a single binding site that matures as it progresses from the ER to the cell membrane. Indeed, the juxtaposition of Co- and Po-activities with **5** versus only Po-activity with **25−27** implies that, in this cyanoquinoline-based series, the CoPo must be able to access a conformation not precluded by the constraints associated with tethering. In addition, this conformation, which is active for Po-activity, must differ from that associated with Co-activity, implying that **5** must also be able to readily access a conformation that is not accessible by **25−27**. The active conformation enabling potentiation is satisfied by (indeed, enabled by) piperazine-constrained cyanoquinolines (e.g., **25−27** are all better potentiators than **5**). Taken together, the tether-differentiated SAR results delineated in Table 1 suggest that (1) a flexible tether and (2) a relatively short bridge between the cyanoquinoline and arylamide moieties are vital for these cyanoquinoline-based CoPo's to adopt the two distinct conformations required for dual Co- and Po-activities.

Are there energetically accessible conformations of **5** and **25−27** that meet these requirements? One such pair of conformers (there may well be others, but these conformers illustrate the point) located by our conformational search calculations are shown in Figure 7, a conformation possibly associated with the Co-activity of **5** at left and a conformation possibly associated with Po-activity for **26** (the molecule in the

(a) (b)
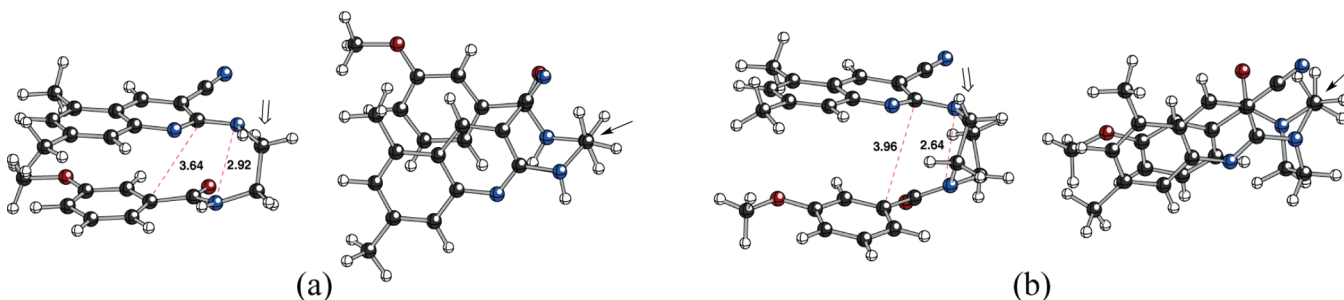
Figure 7. (a) Possible "Co"-active conformer of **5**. (b) Possible "Po"-active conformer of **26**. Two views of each structure are shown. In the left-hand presentation of each structure, the viewing angle is perpendicular to the C−C bond of the tether (downward double-arm arrow); this view emphasizes the differing dihedral angles between the C−N bonds. In the right-hand presentation of each structure, the orientation is systematized by viewing down this same C−C bond (↓). Selected through-space distances are shown in Å.

25−27 series that has the same aryl group as **5**) at right. First, note that both of these conformers are folded to allow for some degree of π-stacking between the quinoline and methoxyphenyl groups, an effect that is perhaps maximized in water. The conformer shown for **26** is predicted to be the lowest energy conformer in water for this molecule (despite the twist-boat conformation of its piperazine core), while that for **5** is predicted to be the seventh-lowest conformer in water, only approximately 3 kcal/mol higher in energy than the lowest energy conformer. Here we focus on a low energy conformer of **5** that could possibly mimic that shown for **26** by undergoing relatively minor conformational changes; the lowest energy conformers predicted for **5** (see Supporting Information), although still displaying π-stacking interactions, do not orient their NH groups in such a way as to allow for such a conformational exchange to occur. Although strong binding to a target can overcome energy penalties associated with nonoptimal conformations of ligands, if the conformer shown for **26** does correspond to the Po-active conformation, no energy penalty associated with changing this conformation from the predominant conformation in water will need to be paid.[18] Since **5** is also active, however, a **26**-like conformation would need to be energetically accessible. Altering the conformation of **5** such that the quinoline and methoxyphenyl groups are in the same relative orientation as in **26** (and allowing the rest of the molecule to relax; see Supporting Information for details) is predicted to be accompanied by an increase in energy of approximately 4 kcal/mol (likely the result of not only disrupting π-stacking but also disrupting the gauche conformation of the N−C−C−N substructure, which is preferred on both steric and orbital-based grounds over other staggered conformations;[19] note that this distorted conformation is predicted to be approximately 8 kcal/mol above the lowest energy conformation of **5** in water). Thus, **5** could adopt the shape of **26** if this energy penalty is not enough to cause dissociation or is counterbalanced by favorable interactions with a binding site cavity complementary to **26**. We see no reason why this relatively small change to the conformation of **5** could not occur within a binding site (i.e., without dissociation) that switches between a Co- and a Po-form, each complementary to one or the other arrangement of the quinoline and methoxyphenyl groups shown in Figure 7a and Figure 7b. Although this model is speculative, it should be testable through synthesis of, and activity assays on, quinolines with further conformational constraints.

Additional structure−activity insight was derived from examination of the arylamide moiety. Substitution at the *ortho* position of the arylamide generally gave worse corrector activity but better potentiator activity (e.g., CoPo's **14**, **16**, **25**, **28**, and **34**). The best corrector activity was seen with an ethylene tether employing a methoxy substitution at either the *meta* (**5**) or *para* (CoPo **15**) position of the arylamide, and the greatest corrector activity was obtained by placing a methoxy substituent at both (CoPo **21**); note that electron-donating methoxy groups may well enhance the preference for π-stacked conformations. A similar trend can be seen with the propylene tether, as CoPo's **32** and **33** are superior correctors compared to **31**. In general, hydrogen bond accepting groups at the *meta* and *para* positions afforded the best corrector activity as exemplified in the propylene diamine series with CoPo's **31**−**36**. Methoxy substitution proved to be superior to nitrogen heterocyclic amides in corrector activity. A hybrid pyridyl-methoxyamide (CoPo **23**) maintained corrector and improved

potentiator activity, while most other modifications giving better corrector or better potentiator activity did so at the expense of the other. These data suggest that dual CoPo activity is not a general feature of cyanoquinolines but is rather dependent on the particular tether and/or arylamide substituent.

CONCLUSION

This work provides structure−activity insight around the unique cyanoquinoline-based CoPo scaffold, which has dual, independent ΔF508-CFTR corrector and potentiator activities. The most active diamine tether was shown to be 1,2-diaminoethane-based compared to more constrained (piperazine) and more flexible (1,3-diaminopropylene) counterparts. Additionally, variations of the arylamide moiety can tune the corrector and/or potentiator activities. This work has led to the hypothesis that cyanoquinoline-based CoPo's have dual activity if they can conformationally adapt to a single binding site that evolves during the endoplasmic reticulum ⇒ cell membrane transition. While the target site(s) of CoPo's remain unknown, this work provides a working hypothesis regarding the corrector and potentiator structural features of the reported cyanoquinoline-based CoPo scaffold.

EXPERIMENTAL SECTION

General Experimental. All purchased starting materials and reagents were used without further purification. Product purification was performed either on an automated flash chromatography system (Combiflash by Teledyne, 35 min of elution with linear gradient from 100% hexane to 100% EtOAc solvent) with silica gel columns or on an HPLC system [Waters, 15 mL/min flow rate, linear gradient elution with 0.1% TFA-containing H_2O/MeCN from 5% to 95% MeCN in 20 min, Xterra Prep MS C18 OBD column (19 mm × 100 mm), and dual wavelength absorbance detector]. NMR spectra (^{1}H at 400 MHz, ^{13}C at 100 MHz) were recorded in $CDCl_3$ solvent on a Varian 600. Chemical shifts are expressed in parts per million relative to solvent. Coupling constants are expressed in units of hertz (Hz). Splitting patterns are designated as s (singlet), d (doublet), t (triplet), q (quartet), m (multiplet), and bs (broad singlet). LC/MS (Waters Micromass ZQ) specifications are as follows: electrospray (+) ionization, mass ranging from 100 to 900 Da, 20 V cone voltage. For LC, the specifcations are Xterra MS C18 column (2.1 mm × 50 mm × 3.5 μm), 0.2 mL/min water/acetonitrile (containing 0.1% TFA), 30 min linear gradient 0−100% acetonitrile. The LC/MS UV detector is a diode array with 200−400 nm wavelength range. Purity is based on integration of peak area as a percentage of the UV diode array signals. Compound purities are determined by RP-HPLC (≥95%).

ΔF508-CFTR Corrector and Potentiator Activity Assays. - *Plate Reader Assay.* FRT cells stably coexpressing human ΔF508-CFTR and the halide-sensing fluorescent protein YFP-H148Q/I152L were used as described previously.[6d] For corrector assay, cells were grown at 37 °C for 24 h and then incubated for 16−20 h with 200 μL of medium containing the test compound. At the time of the assay, cells were washed with PBS and then incubated with PBS containing forskolin (20 μM) and genistein (50 μM) for 20 min. For potentiator assay, cells were grown at 37 °C for 18−24 h and then for 18−24 h at 27 °C. At the time of the assay, cells were washed with PBS and then incubated for 10 min with PBS (50 μL) containing forskolin (20 μM) and test compound (0−50 μM final concentration). Measurements were carried out using FLUOstar fluorescence plate readers (Optima, BMG LABTECH Gmbh), equipped with 500 ± 10 nm excitation and 535 ± 15 nm emission filters. Each well was assayed individually for I⁻ influx by recording fluorescence for 2 s (baseline) and then for 12 s after rapid addition of 165 μL of PBS in which 137 mM Cl⁻ was replaced by I⁻. I⁻ influx rate was computed by exponential regression. All experiments contained negative control (DMSO vehicle) and

positive controls (potentiator assay, genistein; corrector assay, **1**). EC_{50} and V_{max}, and their associated uncertainties, were determined by four-parameter logistic nonlinear regression from concentration–activity data using GraphPad Prism, version 5.01. Initial iodide influx rates were fitted to the Hill equation: activity (initial slope) = $A_o + V_{max}C_i^H / (C_i^H + IC_{50}^H)$, where C_i is compound concentration, H is coefficient, and A_o is background signal.

Short-Circuit Current Measurements. ΔF508-CFTR-expressing FRT cells were cultured on Snapwell inserts for 7–9 days. For corrector assay, test compounds were incubated with cells for 18–24 h at 37 °C prior to measurements. For potentiator assay, the FRT cells were incubated for 18–24 h at 27 °C prior to measurements. Short-circuit current was recorded using established procedures.[6d]

N-(3,5-Dimethylphenyl)acetamide (7). Acetic anhydride (2.84 mL, 30 mmol) was dissolved in dry THF (10 mL), purged with N_2, and brought to 0 °C. 3,5-Dimethylaniline (1.25 mL, 10 mmol) was added dropwise, and upon completion of the addition, the mixture was allowed to warm to room temperature and stirred an additional hour. The reaction solution was then poured over ice, and 1 M NaOH (aq) was added to adjust the pH to 12–14. The precipitate was collected by filtration, dissolved in DCM, and dried over Na_2SO_4. The drying agent was removed by filtration and the solvent was removed under reduced pressure to afford pure product in 99% yield as a white solid.[12]

2-Chloro-5,7-dimethylquinoline-3-carbaldehyde (8). Phosphorus oxychloride (6.52 mL, 70 mmol) and dry DMF (1.94 mL, 25 mmol) were refluxed for 2 h under a N_2 atmosphere. Acetamide **2** (1.632 g, 10 mmol) was then added to the reaction solution as a solid, and the mixture was stirred at room temperature for an additional 3 h. The reaction solution was poured slowly over ice, diluted with water (200 mL), and carefully neutralized with solid K_2CO_3. The precipitate was then collected by filtration, dissolved in chloroform, and dried over Na_2SO_4. The drying agent was removed by filtration and the solvent was removed under reduced pressure to afford pure product in 95% yield as an orange solid.[12]

2-Chloro-5,7-dimethylquinoline-3-carbonitrile (10). Aldehyde **8** (1.095 g, 5 mmol), hydroxylamine hydrochloride (0.365 g, 5.25 mmol), and triethylamine (1.00 mL, 7 mmol) were combined in ethanol (50 mL). The solution was refluxed for 3 h, and then the ethanol was removed under reduced pressure. Aqueous HCl (1M, 100 mL) was added to the crude material, and product was extracted with DCM (100 mL). The organic layer was separated and dried over Na_2SO_4. The drying agent was filtered and solvent was removed under reduced pressure. The crude product **4** was then dissolved in dry benzene (50 mL). Thionyl chloride (0.73 mL, 10 mmol) was added dropwise to the solution, and the mixture was refluxed under a N_2 atmosphere for 4 h. The solution was allowed to cool to room temperature. Then the benzene and excess thionyl chloride were removed under reduced pressure to afford pure product **5** in 93% yield as a light brown solid. ^{1}H NMR (400 MHz, CDCl₃) δ 8.62 (s, 1H), 7.62 (s, 1H), 7.33 (s, 1H), 2.66 (s, 3H), 2.54 (s, 3H).

General Procedure for Aromatic Substitution of 5 with Diamine Tether (11–13). Carbonitrile **5** (1.083 g, 5 mmol) and diamine (15 mmol) were refluxed in dioxane (50 mL) until judged complete by TLC. The mixture was allowed to cool to room temperature, and dioxane was removed under reduced pressure. The crude product was suspended in NH_4Cl (1 M, aq) and collected by filtration. The solids were washed with diethyl ether and allowed to dry on a filter paper under vacuum. Yields ranged from 40% to 80%.

2-((2-Aminoethyl)amino)-5,7-dimethylquinoline-3-carbonitrile (11). ^{1}H NMR (400 MHz, CDCl3) δ 8.31 (s, 1H), 7.32 (s, 1H), 6.92 (s, 1H), 5.64 (t, *J* = 4.8, 1H), 3.65 (q, *J* = 5.7, 2H), 3.01 (t, *J* = 6.0, 2H), 2.52 (s, 3H), 2.42 (s, 3H).[8]

2-(3-Aminopropylamino)-5,7-dimethylquinoline-3-carbonitrile (12). Yellow solid. Yield: 61%. ^{1}H NMR (600 MHz, CDCl₃) δ 8.30 (s, 1H), 7.32 (s, 1H), 6.91 (s, 1H), 6.18 (s, 1H), 3.72 (q, *J* = 6.2, 2H), 2.89 (t, *J* = 6.2, 2H), 2.52 (s, 3H), 2.42 (s, 3H), 1.82 (quint, *J* = 6.4, 2H), 1.64 (s, 2H); ^{13}C NMR (150 MHz, CDCl₃) δ 154.56, 150.37, 143.73, 140.41, 135.13, 126.48, 124.52, 118.89, 117.41, 94.14, 40.40, 40.05, 32.52, 22.20, 18.53. ESI-MS *m/z* [M + H]⁺: 255.33. Purity: 99%.

5,7-Dimethyl-2-(piperazin-1-yl)quinoline-3-carbonitrile (13). Orange solid. Yield: 62%. ^{1}H NMR (600 MHz, CDCl₃) δ 8.35 (d, *J* = 4.1, 1H), 7.35 (s, 1H), 6.95 (s, 1H), 3.60 (m, 4H), 3.02 (m, 4H), 2.49 (s, 3H), 2.40 (s, 3H), 1.87 (s, 1H); ^{13}C NMR (150 MHz, CDCl₃) δ 158.00, 149.29, 143.62, 142.63, 134.79, 127.89, 125.21, 120.08, 118.47, 97.37, 50.30, 46.16, 22.23, 18.47. ESI-MS *m/z* [M + H]⁺: 267.28. Purity: 99%.

General Procedure for Amide Coupling Reactions. EDC hydrochloride (0.192 g, 1 mmol), aryl acid (1 mmol), and triethylamine (0.14 mL, 2.5 mmol) were dissolved in dry DCM (10 mL). The mixture was stirred at room temperature for 30 min. Carbonitrile (1 mmol) dissolved in dry DCM (5 mL) was added dropwise to the solution, and the mixture was stirred for 18 h. The mixture was diluted with DCM (50 mL) and washed with 1 M $NaHSO_4$ (aq, 2 × 100 mL). Organics were dried over Na_2SO_4, filtered, and the solvent was removed under reduced pressure. The crude product was purified by flash chromatography. Characterization data can be found in the Supporting Information for all final compounds.

N-(2-((3-Cyano-5,7-dimethylquinolin-2-yl)amino)ethyl)-2-methoxybenzamide (14). Yellow solid. Yield 72%. ^{1}H NMR (600 MHz, CDCl₃) δ 8.31 (s, 1H), 8.24–8.17 (m, 2H), 7.41 (t, *J* = 7.4, 1H), 7.30 (s, 1H), 7.06 (t, *J* = 7.4, 1H), 6.96–6.88 (m, 2H), 5.85 (s, 1H), 3.90–3.78 (m, 9H), 2.52 (s, 3H), 2.41 (s, 3H); ^{13}C NMR (150 MHz, CDCl₃) δ 166.69, 157.65, 154.31, 143.81, 140.49, 135.15, 133.00, 132.45, 131.07, 128.98, 126.76, 124.66, 121.49, 119.08, 117.09, 111.45, 94.37, 56.13, 42.05, 39.91, 22.31, 18.82. ESI-MS *m/z* [M + H]⁺: 375.18. Purity: 98%.

N-(2-((3-Cyano-5,7-dimethylquinolin-2-yl)amino)ethyl)-4-methoxybenzamide (15). Yellow solid. Yield: 72%. ^{1}H NMR (600 MHz, CDCl₃) δ 8.26 (s, 1H), 7.87 (s, 1H), 7.61 (d, *J* = 8.0, 2H), 7.24 (s, 1H), 6.90 (s, 1H), 6.67 (d, *J* = 8.7, 2H), 5.80 (s, 1H), 3.83 (q, *J* = 5.2, 3H), 3.70 (s, 3H), 3.67 (q, *J* = 5.2, 2H), 2.46 (s, 3H), 2.37 (s, 3H); ^{13}C NMR (150 MHz, CDCl₃) δ 167.82, 162.18, 155.18, 149.70, 144.14, 140.93, 135.45, 132.48, 129.16, 127.12, 124.50, 119.39, 116.87, 113.66, 94.49, 55.43, 43.09, 41.29, 22.15, 18.47. ESI-MS *m/z* [M + H]⁺: 375.18. Purity: 98%.

N-(2-((3-Cyano-5,7-dimethylquinolin-2-yl)amino)ethyl)-picolinamide (16). Yellow solid. Yield: 60%. ^{1}H NMR (600 MHz, CDCl₃) δ 8.87 (s, 1H), 8.43–8.41 (m, 1H), 8.32 (s, 1H), 8.20 (d, *J* = 7.8, 1H), 7.81 (td, *J* = 7.7, 1.7, 1H), 7.49 (s, 1H), 7.40–7.35 (m, 1H), 6.95 (s, 1H), 5.78 (s, 1H), 3.91 (dd, *J* = 11.3, 5.7, 2H), 3.81 (dd, *J* = 11.2, 5.6, 2H), 2.53 (s, 3H), 2.47 (s, 3H); ^{13}C NMR (150 MHz, CDCl₃) δ 165.40, 154.49, 150.13, 148.14, 143.59, 140.55, 137.44, 135.08, 126.82, 126.28, 125.02, 122.49, 119.24, 117.07, 94.17, 41.66, 40.86, 22.30, 18.53. ESI-MS *m/z* [M + H]⁺: 346.16. Purity: 96%.

N-(2-((3-Cyano-5,7-dimethylquinolin-2-yl)amino)ethyl)-nicotinamide (17). Yellow solid. Yield: 66%. ^{1}H NMR (600 MHz, CDCl₃) δ 8.93 (s, 1H), 8.66 (d, *J* = 4.6, 1H), 8.38 (s, 1H), 8.34 (s, 1H), 8.00 (d, *J* = 7.8, 1H), 7.24–7.20 (m, 2H), 7.00 (s, 1H), 5.79 (s, 1H), 3.94 (q, *J* = 5.6, 2H), 3.77 (q, *J* = 4.3, 2H), 2.56 (s, 3H), 2.43 (s, 3H); ^{13}C NMR (150 MHz, CDCl₃) δ 166.28, 155.17, 152.18, 148.59, 144.58, 141.05, 135.54, 135.18, 130.46, 127.41, 124.24, 123.35, 119.45, 116.77, 94.37, 43.57, 41.25, 22.26, 18.55. ESI-MS *m/z* [M + H]⁺: 346.16. Purity: 97%.

N-(2-((3-Cyano-5,7-dimethylquinolin-2-yl)amino)ethyl)-isonicotinamide (18). Yellow solid. Yield: 69%. ^{1}H NMR (600 MHz, CDCl₃) δ 8.53–8.46 (m, 3H), 8.33 (s, 1H), 7.45 (d, *J* = 4.5, 2H), 7.17 (s, 1H), 6.96 (s, 1H), 5.71 (s, 1H), 3.88 (q, *J* = 5.4, 2H), 3.68 (q, *J* = 5.0, 2H), 2.51 (s, 3H), 2.38 (s, 3H); ^{13}C NMR (151 MHz, CDCl₃) δ 166.03, 155.37, 150.49, 144.68, 141.89, 141.18, 135.74, 127.49, 124.18, 121.36, 119.54, 116.72, 113.58, 94.48, 77.43, 77.22, 77.01, 44.14, 41.00, 22.27, 18.56. ESI-MS *m/z* [M + H]⁺: 346.16. Purity: 98%.

N-(2-((3-Cyano-5,7-dimethylquinolin-2-yl)amino)ethyl)-benzamide (19). Yellow solid. Yield: 84%. ^{1}H NMR (600 MHz, CDCl₃) δ 8.35 (s, 1H), 8.14 (s, 1H), 7.71 (d, *J* = 8.0, 2H), 7.41 (t, *J* = 7.4, 1H), 7.28 (s, 1H), 7.26 (t, *J* = 5.5, 1H), 6.98 (s, 1H), 5.82 (t, *J* = 5.5, 1H), 3.91 (q, *J* = 5.7, 2H), 3.75 (q, *J* = 4.6, 2H), 2.54 (s, 3H), 2.43 (s, 3H); ^{13}C NMR (151 MHz, CDCl₃) δ 168.16, 155.19, 149.55, 144.15, 140.96, 135.46, 131.40, 130.30, 128.49, 127.40, 127.15, 124.46,

119.40, 116.89, 94.37, 43.40, 41.25, 22.24, 18.60. ESI-MS *m/z* [M + H]⁺: 345.12. Purity: 99%.

N-(2-((3-Cyano-5,7-dimethylquinolin-2-yl)amino)ethyl)-2,4-dimethoxybenzamide (20). Yellow solid. Yield: 52%. ¹H NMR (600 MHz, CDCl₃) δ 8.28 (s, 1H), 8.18 (d, *J* = 8.7, 1H), 8.04 (s, 1H), 7.29 (s, 1H), 6.91 (s, 1H), 6.57 (dd, *J* = 8.8, 2.2, 1H), 6.40 (d, *J* = 2.1, 1H), 5.87 (s, 1H), 3.86–3.76 (m, 10H), 2.51 (s, 3H), 2.40 (s, 3H); ¹³C NMR (150 MHz, CDCl₃) δ 166.26, 163.58, 159.00, 154.31, 150.21, 143.68, 140.37, 135.08, 134.17, 126.67, 124.71, 119.05, 117.09, 114.68, 105.41, 98.69, 94.18, 56.06, 55.70, 42.11, 39.57, 22.21, 18.52. ESI-MS *m/z* [M + H]⁺: 405.15. Purity: 98%.

N-(2-((3-Cyano-5,7-dimethylquinolin-2-yl)amino)ethyl)-3,4-dimethoxybenzamide (21). Yellow solid. Yield: 41%. ¹H NMR (600 MHz, CDCl₃) δ 8.37 (s, 1H), 7.89 (s, 1H), 7.36 (d, *J* = 1.8, 1H), 7.29 (s, 1H), 7.18 (dd, *J* = 8.3, 1.9, 1H), 6.99 (s, 1H), 6.65 (d, *J* = 8.3, 1H), 5.78 (s, 1H), 3.92 (q, *J* = 5.8, 2H), 3.86 (s, 3H), 3.78 (s, 3H), 3.75 (q, *J* = 5.3, 2H), 2.56 (s, 3H), 2.43 (s, 3H); ¹³C NMR (150 MHz, CDCl₃) δ 168.07, 155.20, 151.72, 149.68, 149.04, 144.18, 140.94, 135.52, 127.57, 127.11, 124.58, 119.87, 119.40, 116.89, 110.89, 110.24, 94.37, 56.11, 56.09, 43.14, 41.37, 22.25, 18.59. ESI-MS *m/z* [M + H]⁺: 405.15. Purity: 98%.

N-(2-((3-Cyano-5,7-dimethylquinolin-2-yl)amino)ethyl)-pyrazine-2-carboxamide (22). Yellow solid. Yield: 38%. ¹H NMR (600 MHz, CDCl₃) δ 9.36 (s, 1H), 8.94 (s, 1H), 8.66–8.65 (m, 1H), 8.32 (s, 1H), 8.32–8.30 (m, 1H), 7.48 (s, 1H), 6.96 (s, 1H), 5.76 (s, 1H), 3.92 (q, *J* = 5.0, 2H), 3.80 (q, *J* = 5.2, 2H), 2.53 (s, 3H), 2.47 (s, 3H); ¹³C NMR (150 MHz, CDCl₃) δ 163.98, 154.64, 149.96, 147.22, 144.85, 144.53, 143.61, 142.56, 140.67, 135.19, 126.93, 124.93, 119.32, 116.98, 94.15, 41.66, 41.17, 22.35, 18.53. ESI-MS *m/z* [M + H]⁺: 376.12. Purity: 97%.

N-(2-((3-Cyano-5,7-dimethylquinolin-2-yl)amino)ethyl)-5-methoxypicolinamide (23). Yellow solid. Yield: 78%. ¹H NMR (600 MHz, CDCl₃) δ 8.69 (s, 1H), 8.29 (s, 1H), 8.13 (d, *J* = 8.6, 1H), 8.05 (d, *J* = 2.8, 1H), 7.47 (s, 1H), 7.22 (dd, *J* = 8.6, 2.9, 1H), 6.93 (s, 1H), 5.81 (t, *J* = 5.5, 1H), 3.88 (q, *J* = 5.5, 2H), 3.85 (s, 3H), 3.78 (q, *J* = 5.6, 2H), 2.51 (s, 3H), 2.46 (s, 3H); ¹³C NMR (150 MHz, CDCl₃) δ 165.32, 157.93, 154.51, 150.12, 143.50, 142.88, 140.49, 136.52, 135.06, 126.74, 125.02, 123.58, 120.18, 119.19, 117.08, 94.16, 55.88, 41.73, 40.79, 22.31, 18.52. ESI-MS *m/z* [M + H]⁺: 376.12. Purity: 99%.

N-(2-((3-Cyano-5,7-dimethylquinolin-2-yl)amino)ethyl)-2,6-dimethoxybenzamide (24). ¹H NMR (600 MHz, CDCl₃) δ 8.30 (s, 1H), 7.26 (t, *J* = 4.3, 1H), 7.22 (t, *J* = 8.4, 1H), 6.98 (s, 1H), 6.90 (s, 1H), 6.49 (d, *J* = 8.4, 2H), 5.69 (t, *J* = 5.6, 1H), 3.85 (q, *J* = 5.6, 2H), 3.74 (q, *J* = 4.9, 2H), 3.69 (s, 6H), 2.51 (s, 3H), 2.33 (s, 3H); ¹³C NMR (150 MHz, CDCl₃) δ 166.38, 157.60, 154.45, 149.77, 143.85, 140.52, 135.05, 130.63, 126.84, 124.35, 119.10, 116.95, 116.35, 104.15, 94.19, 56.15, 41.58, 41.35, 22.17, 18.47. ESI-MS *m/z* [M + H]⁺: 405.15. Purity: 99%.

2-(4-(2-Methoxybenzoyl)piperazin-1-yl)-5,7-dimethylquinoline-3-carbonitrile (25). Yellow solid. Yield: 40%. ¹H NMR (600 MHz, CDCl₃) δ 8.47 (s, 1H), 7.44 (s, 1H), 7.37 (t, *J* = 7.9, 1H), 7.28 (m, 1H), 7.07 (s, 1H), 7.01 (t, *J* = 7.4, 1H), 6.94 (d, *J* = 8.3, 1H), 4.03 (m, 2H), 3.85 (s, 3H), 3.76 (dd, *J* = 6.4, 10.8, 2H), 3.54 (m, 4H), 2.58 (s, 3H), 2.47 (s, 3H); ¹³C NMR (150 MHz, CDCl₃) δ 168.23, 157.75, 155.51, 149.20, 144.02, 142.73, 134.97, 130.82, 128.44, 128.29, 125.72, 125.36, 121.24, 120.47, 118.22, 111.13, 97.67, 55.80, 49.62, 48.95, 46.90, 41.69, 22.29, 18.54. ESI-MS *m/z* [M + H]⁺: 401.13. Purity: 93%.

2-(4-(3-Methoxybenzoyl)piperazin-1-yl)-5,7-dimethylquinoline-3-carbonitrile (26). Yellow solid. Yield: 50%. ¹H NMR (600 MHz, CDCl₃) δ 8.49 (s, 1H), 7.44 (s, 1H), 7.33 (td, *J* = 1.4, 7.4, 1H), 7.08 (s, 1H), 6.98 (m, 3H), 3.83 (s, 3H), 3.76 (m, 8H), 2.58 (s, 3H), 2.47 (s, 3H); ¹³C NMR (150 MHz, CDCl₃) δ 170.51, 159.92, 157.76, 149.15, 144.05, 142.69, 137.10, 134.99, 129.90, 128.54, 125.40, 120.55, 119.30, 118.14, 115.93, 112.64, 97.77, 55.59, 49.59, 49.18, 47.71, 42.20, 29.91, 22.29, 18.54. ESI-MS *m/z* [M + H]⁺: 401.26. Purity: 99%.

2-(4-(4-Methoxybenzoyl)piperazin-1-yl)-5,7-dimethylquinoline-3-carbonitrile (27). Yellow solid. Yield: 45%. ¹H NMR (600 MHz, CDCl₃) δ 8.47 (s, 1H), 7.44 (m, 3H), 7.07 (s, 1H), 6.94 (d, *J* = 8.8, 2H), 3.84 (s, 8H), 3.83 (m, 8H), 2.57 (s, 3H), 2.47 (s, 3H); ¹³C

NMR (150 MHz, CDCl₃) δ 170.48, 161.10, 157.75, 149.16, 144.02, 142.69, 134.98, 129.43, 128.49, 127.82, 125.38, 120.51, 118.18, 114.00, 97.72, 55.62, 49.33, 29.91, 22.29, 21.60, 18.86, 18.53. ESI-MS *m/z* [M + H]⁺: 401.13. Purity: 93%.

5,7-Dimethyl-2-(4-picolinoylpiperazin-1-yl)quinoline-3-carbonitrile (28). Yellow Solid. Yield: 40%. ¹H NMR (600 MHz, CDCl₃) δ 8.62 (d, *J* = 4.8, 1H), 8.48 (s, 1H), 7.83 (t, *J* = 8.4, 1H), 7.71 (d, *J* = 7.8, 1H), 7.43 (s, 1H), 7.38 (dd, *J* = 5.2, 7.2, 1H), 7.07 (s, 1H), 3.85 (m, 8H), 2.58 (s, 3H), 2.47 (s, 3H); ¹³C NMR (150 MHz, CDCl₃) δ 167.89, 157.64, 154.06, 149.20, 148.56, 143.99, 142.74, 137.36, 134.94, 128.41, 125.38, 124.86, 124.28, 120.46, 118.25, 97.55, 49.58, 48.82, 47.23, 42.46, 22.28, 18.53. ESI-MS *m/z* [M + H]⁺: 360.24. Purity: 99%.

5,7-Dimethyl-2-(4-nicotinoylpiperazin-1-yl)quinoline-3-carbonitrile (29). Yellow solid. Yield: 49%. ¹H NMR (600 MHz, CDCl₃) δ 8.73 (s, 1H), 8.70 (d, *J* = 3.7, 1H), 8.50 (s, 1H), 7.81 (d, *J* = 7.8, 1H), 7.45 (s, 1H), 7.40 (dd, *J* = 4.9, 7.8, 1H), 7.09 (s, 1H), 4.02 (s, 2H), 3.70 (m, 6H), 2.59 (s, 3H), 2.48 (s, 3H); ¹³C NMR (150 MHz, CDCl₃) δ 168.14, 157.66, 151.16, 149.09, 148.25, 144.13, 142.70, 135.29, 135.01, 131.64, 128.66, 125.42, 123.73, 120.62, 118.07, 97.80, 49.42, 49.15, 47.79, 42.35, 22.29, 18.54. ESI-MS *m/z* [M + H]⁺: 360.31. Purity: 99%.

2-(4-Isonicotinoylpiperazin-1-yl)-5,7-dimethylquinoline-3-carbonitrile (30). Yellow solid. Yield: 50%. ¹H NMR (600 MHz, CDCl₃) δ 8.74 (d, *J* = 5.6, 2H), 8.50 (s, 1H), 7.45 (s, 1H), 7.34 (d, *J* = 5.8, 2H), 7.10 (s, 1H), 4.01 (s, 2H), 3.76 (s, 2H), 3.61 (s, 4H), 2.59 (s, 3H), 2.48 (s, 3H); ¹³C NMR (150 MHz, CDCl₃) δ 168.10, 157.67, 150.62, 149.08, 144.16, 143.40, 142.70, 135.03, 128.71, 125.42, 121.45, 120.65, 118.04, 97.85, 49.45, 49.12, 47.45, 42.08, 22.30, 18.55. ESI-MS *m/z* [M + H]⁺: 360.31. Purity: 99%.

N-(3-(3-Cyano-5,7-dimethylquinolin-2-ylamino)propyl)-2-methoxybenzamide (31). Yellow solid. Yield: 88%. ¹H NMR (600 MHz, CDCl₃) δ 8.28 (s, 1H), 8.21 (t, *J* = 5.3, 1H), 8.18 (dd, *J* = 1.8, 7.8, 1H), 7.44 (td, *J* = 1.8, 8.4, 1H), 7.20 (s, 1H), 7.07 (t, *J* = 7.9, 1H), 6.97 (d, *J* = 8.2, 1H), 6.89 (s, 1H), 5.76 (t, *J* = 5.7, 1H), 3.92 (s, 4H), 3.74 (q, *J* = 6.3, 2H), 3.59 (q, *J* = 6.2, 2H), 2.51 (s, 3H), 2.36 (s, 3H), 1.98 (m, 2H); ¹³C NMR (150 MHz, CDCl₃) δ 166.01, 157.51, 154.46, 150.24, 143.66, 140.43, 135.16, 132.75, 132.37, 126.51, 124.41, 122.32, 121.44, 118.93, 117.23, 111.40, 94.16, 56.11, 38.60, 37.11, 30.17, 22.25, 18.55. ESI-MS *m/z* [M + H]⁺: 389.32. Purity: 99%.

N-(3-(3-Cyano-5,7-dimethylquinolin-2-ylamino)propyl)-3-methoxybenzamide (32). Yellow solid. Yield: 87%. ¹H NMR (600 MHz, CDCl₃) δ 8.30 (s, 1H), 7.66 (t, *J* = 6.0, 1H), 7.42 (m, 2H), 7.35 (t, *J* = 7.9, 1H), 7.11 (s, 1H), 7.06 (dd, *J* = 2.5, 8.1, 1H), 6.90 (s, 1H), 5.65 (t, *J* = 6.3, 1H), 3.83 (s, 2H), 3.80 (dd, *J* = 6.3, 12.2, 2H), 3.51 (dd, *J* = 6.1, 12.0, 2H), 2.51 (s, 3H), 2.30 (s, 3H), 1.92 (m, 2H); ¹³C NMR (150 MHz, CDCl₃) δ 168.26, 159.97, 154.81, 149.96, 144.07, 140.81, 137.26, 135.35, 129.67, 126.72, 124.17, 119.32, 119.01, 117.62, 117.14, 112.70, 94.10, 55.60, 37.89, 36.37, 30.43, 30.42, 22.12, 18.54. ESI-MS *m/z* [M + H]⁺: 389.32. Purity: 99%.

N-(3-(3-Cyano-5,7-dimethylquinolin-2-ylamino)propyl)-4-methoxybenzamide (33). Yellow solid. Yield: 81%. ¹H NMR (600 MHz, CDCl₃) δ 8.30 (s, 1H), 7.83 (d, *J* = 8.6, 2H), 7.50 (s, 1H), 7.20 (s, 1H), 6.92 (m, 3H), 5.77 (s, 1H), 3.84 (s, 3H), 3.80 (dd, *J* = 5.9, 11.8, 2H), 3.51 (dd, *J* = 6.1, 11.9, 2H), 2.51 (s, 3H), 2.34 (s, 3H), 1.93 (m, 2H); ¹³C NMR (150 MHz, CDCl₃) δ 167.96, 162.21, 154.61, 135.47, 130.31, 129.31, 128.52, 127.87, 127.25, 126.78, 124.01, 118.85, 117.05, 113.91, 94.27, 55.61, 38.14, 36.46, 30.32, 22.22, 18.55. ESI-MS *m/z* [M + H]⁺: 389.32. Purity: 99%.

N-(3-(3-Cyano-5,7-dimethylquinolin-2-ylamino)propyl)-picolinamide (34). Yellow solid. Yield: 42%. ¹H NMR (600 MHz, CDCl₃) δ 8.72 (s, 1H), 8.58 (d, *J* = 4.2, 1H), 8.27 (s, 1H), 8.18 (d, *J* = 7.8, 1H), 7.80 (td, *J* = 1.7, 7.7, 1H), 7.59 (s, 1H), 7.39 (ddd, *J* = 1.1, 4.7, 7.5, 1H), 6.87 (s, 1H), 5.56 (t, *J* = 5.9, 1H), 3.70 (q, *J* = 6.2, 2H), 3.51 (q, *J* = 6.4, 2H), 2.48 (s, 3H), 2.36 (s, 3H), 1.89 (quint, *J* = 6.2, 2H); ¹³C NMR (150 MHz, CDCl₃) δ 167.44, 164.92, 154.65, 150.40, 148.15, 143.70, 140.54, 137.55, 135.13, 126.65, 126.32, 124.84, 122.67, 119.08, 117.24, 94.09, 38.25, 36.50, 30.60, 22.33, 18.55. ESI-MS *m/z* [M + H]⁺: 372.24. Purity: 99%.

N-(3-(3-Cyano-5,7-dimethylquinolin-2-ylamino)propyl)-nicotinamide (35). Yellow solid. Yield: 40%. ¹H NMR (600 MHz,

CDCl$_3$) δ 9.09 (s, 1H), 8.77 (d, J = 6.3, 1H), 8.34 (s, 1H), 8.15 (d, J = 7.9, 1H), 7.70 (s, 2H), 7.41 (dd, J = 4.8, 7.8, 1H), 7.03 (s, 1H), 6.92 (s, 1H), 5.51 (t, J = 6.4, 1H), 3.82 (s, 2H), 3.53 (s, 2H), 2.53 (s, 3H), 2.31 (s, 3H), 1.94 (quint, J=5.5, 2H); ^{13}C NMR (150 MHz, CDCl$_3$) δ 166.37, 154.83, 152.30, 149.84, 148.46, 144.32, 140.91, 135.50, 135.49, 131.46, 126.91, 124.03, 123.64, 119.11, 117.03, 94.19, 37.89, 36.43, 30.41, 22.18, 18.53. ESI-MS m/z [M + H]$^+$: 372.24. Purity: 99%.

N-(3-(3-Cyano-5,7-dimethylquinolin-2-ylamino)propyl)-isonicotinamide (36). Yellow solid. Yield: 42%. ^{1}H NMR (600 MHz, CDCl$_3$) δ 8.70 (d, J = 4.4, 2H), 8.28 (s, 1H), 7.73 (s, 1H), 7.61 (dd, J = 1.6, 4.3, 2H), 6.92 (s, 1H), 6.87 (s, 1H), 5.43 (d, J = 6.0, 1H), 3.76 (q, J = 6.3, 2H), 3.46 (q, J = 5.8, 2H), 2.47 (s, 3H), 2.23 (s, 3H), 1.87 (m, 2H); ^{13}C NMR (150 MHz, CDCl$_3$) δ 166.36, 154.88, 150.74, 149.78, 144.33, 142.93, 140.96, 135.62, 126.97, 123.86, 121.50, 119.15, 116.95, 94.26, 37.84, 36.40, 30.40, 22.20, 18.54. ESI-MS m/z [M + H]$^+$: 372.24. Purity: 99%.

■ ASSOCIATED CONTENT

Ⓢ Supporting Information

ΔF508-CFTR corrector and potentiator activity assay experimentals; experimental details and compound characterization data for compounds **7**, **8**, **10**, and **14−36**; constrained calculation for **5**; coordinates for computed conformers of **5**; and coordinates for computed conformers of **26**. This material is available free of charge via the Internet at http://pubs.acs.org.

■ AUTHOR INFORMATION

Corresponding Author
*Phone: 530-554-2145. Fax: 530-752-8995. E-mail: mjkurth@ucdavis.edu.

■ ACKNOWLEDGMENTS

■ ABBREVIATIONS USED

CF, cystic fibrosis; CFTR, cystic fibrosis transmembrane conductance regulator; ΔF508-CFTR, deletion of phenylalanine-508 in cystic fibrosis transmembrane conductance regulator; CoPo, corrector and potentiator; THF, tetrahydrofuran; DMF, dimethylformamide; DCM, dichloromethane; EDC, 1-ethyl-3-(3-dimethylaminopropyl)carbodiimide hydrochloride; LCMS, liquid chromatography−mass spectrometry

■ REFERENCES

(1) (a) Dalemans, W.; Barbry, P.; Champigny, G.; Jallat, S.; Dott, K.; Dreyer, D.; Crystal, R. G.; Pavirani, A.; Lecocq, J. P.; Lazdunski, M. Altered chloride ion channel kinetics associated with ΔF508 cystic fibrosis mutation. *Nature* **1991**, *354*, 526−528. (b) Snouwaert, J. N.; Brigman, K. K.; Latour, A. M.; Malouf, N. N.; Boucher, R. C.; Smithies, O.; Koller, B. H. An animal model for cystic fibrosis made by gene targeting. *Science* **1992**, *257*, 1083−1088. (c) Boucher, R. C. Cystic fibrosis: a disease of vulnerability to airway surface dehydration. *Trends Mol. Med.* **2007**, *13*, 231−240. (d) Okiyoneda, T.; Barriere, H.; Bagdany, M.; Rabeh, W. M.; Du, K.; Hohfeld, J.; Young, J. C.; Lukacs, G. L. Peripheral protein quality control removes unfolded CFTR from the plasma membrane. *Science* **2010**, *329*, 805−810.

(2) (a) Pilewski, J. M.; Frizzell, R. A. Role of CFTR in airway disease. *Phys. Rev.* **1999**, *79*, S215−S255. (b) Sheppard, D. N.; Welsh, M. J. Structure and function of the CFTR chloride channel. *Physiol. Rev.*

1999, *79*, S23−S45. (c) Zeiher, B. G.; Eichwald, E.; Zabner, J.; Smith, J. J.; Puga, A. P.; McCray, P. B. Jr.; Capecchi, M. R.; Welsh, M. J.; Thomas, K. R. A mouse model for the ΔF508 allele of cystic fibrosis. *J. Clin. Invest.* **1995**, *96*, 2051−2064.

(3) (a) Bobadilla, J. L.; Macek, M; Fine, J. P.; Farrell, P. M. Cystic fibrosis: a worldwide analysis of CFTR mutations-correlation with incidence data and application to screening. *Hum. Mutat.* **2002**, *19*, 575−606. (b) Sharma, M.; Benharouga, M.; Hu, W.; Lukacs, G. L. Conformational and temperature-sensitive stability defects of the ΔF508 cystic fibrosis transmembrane conductance regulator in post-endoplasmic reticulum compartments. *J. Biol. Chem.* **2001**, *276*, 8942−8950. (c) Thibodeau, P. H.; Richardson, J. M.; Wang, W.; Millen, L.; Watson, J.; Mendoza, J. L.; Du, K.; Fischman, S.; Senderowitz, H.; Lukacs, G. L.; Kirk, K.; Thomas, P. J. The cystic fibrosis-causing mutation ΔF508 affects multiple steps in cystic fibrosis transmembrane conductance regulator biogenesis. *J. Biol. Chem.* **2010**, *285*, 35825−35835.

(4) (a) Skach, W. R. Defects in processing and trafficking of the cystic fibrosis transmembrane conductance regulator. *Kidney Int.* **2000**, *57*, 825−831. (b) Denning, G. M.; Anderson, M. P.; Amara, J. F.; Marshall, J.; Smith, A. E.; Welsh, M. J. Processing of mutant cystic fibrosis transmembrane conductance regulator is temperature-sensitive. *Nature* **1992**, *358*, 761−764. (c) Lukacs, G. L.; Mohamed, A.; Kartner, N.; Chang, X.-B.; Riordan, J. R.; Grinstein, S. Conformational maturation of CFTR but not its mutant counterpart (ΔF508) occurs in the endoplasmic reticulum and requires ATP. *EMBO J.* **1994**, *13*, 6076−6086. (d) Kopito, R. R. Biosynthesis and degradation of CFTR. *Physiol. Rev.* **1999**, *79*, S167−S173. (e) Du, K.; Sharma, M.; Lukacs, G. L. The ΔF508 cystic fibrosis mutation impairs domain−domain interactions and arrests post-translational folding of CFTR. *Nat. Struct. Mol. Biol.* **2005**, *12*, 17−25.

(5) Drug discovery reviews: (a) Riordan, J. R. CFTR function and prospects for therapy. *Annu. Rev. Biochem.* **2008**, *77*, 701−726. (b) Verkman, A. S.; Galietta, L. J. Chloride channels as drug targets. *Nat. Rev. Drug Discovery* **2009**, *8*, 153−171.

(6) (a) Yoo, C. L.; Yu, G. J.; Yang, B.; Robins, L. I.; Verkman, A. S.; Kurth, M. J. 4′-Methyl-4,5′-bithiazole-based correctors of defective ΔF508-CFTR cellular processing. *Bioorg. Med. Chem. Lett.* **2008**, *18*, 2610−2614. (b) Yu, G. J.; Yoo, C. L.; Yang, B.; Lodewyk, M. W.; Meng, L.; El-Idreesy, T. T.; Fettinger, J. C.; Tantillo, D. J.; Verkman, A. S.; Kurth, M. J. Potent s-cis-Locked Bithiazole Correctors of ΔF508 Cystic Fibrosis Transmembrane Conductance Regulator Cellular Processing for Cystic Fibrosis Therapy. *J. Med. Chem.* **2008**, *51*, 6044−6054. (c) Ye, L.; Knapp, J. M.; Sangwung, P.; Fettinger, J. C.; Verkman, A. S.; Kurth, M. J. Pyrazolylthiazole as ΔF508-Cystic Fibrosis Transmembrane Conductance Regulator Correctors with Improved Hydrophilicity Compared to Bithiazoles. *J. Med. Chem.* **2010**, *53*, 3772−3781. (d) Pedemonte, N.; Lukacs, G. L.; Du, K.; Caci, E.; Zegarra-Moran, O.; Galietta, L. J.; Verkman, A. S. Small-molecule correctors of defective ΔF508-CFTR cellular processing identified by high-throughput screening. *J. Clin. Invest.* **2005**, *115*, 2564−2571. (e) Noel, S.; Wilke, M.; Bot, A. G.; De Jonge, H. R.; Becq, F. Parallel improvement of sodium and chloride transport defects by miglustat (n-butyldeoxynojyrimicin) in cystic fibrosis epithelial cells. *J. Pharmacol. Exp. Ther.* **2008**, *325*, 1016−1023. (f) Van Goor, F.; Hadida, S.; Grootenhuis, P. D.; Stack, J. H.; Burton, B.; Olson, E.; Wine, J.; Frizzell, R. A.; Ashlock, M.; Negulescu, P. Rescue of the protein folding defect in cystic fibrosis in vitro by the investigational small molecule, VX-809. *J. Cystic Fibrosis* **2010**, *9*, S14. (g) Pedemonte, N.; Tomati, V.; Sondo, E.; Caci, E.; Millo, E.; Armirotti, A.; Damonte, G.; Zegarra-Moran, O.; Galietta, L. J. Dual activity of amino-arylthiazoles on the trafficking and gating defects of the cystic fibrosis transmembrane conductance regulator chloride channel caused by cystic fibrosis mutations. *J. Biol. Chem.* **2011**, *286*, 15215−15226. (h) Wang, Y.; Loo, T. W.; Bartlett, M. C.; Clarke, D. M. Modulating the folding of P-glycoprotein and cystic fibrosis transmembrane conductance regulator truncation mutants with pharmacological chaperones. *Mol. Pharmacol.* **2007**, *71*, 751−758.

(7) (a) Pedemonte, N.; Boido, D.; Moran, O.; Giampieri, M.; Mazzei, M.; Ravazzolo, R.; Galietta, L. J. Structure−activity relationship of 1,4-dihydropyridines as potentiators of the cystic fibrosis transmembrane conductance regulator chloride channel. *Mol. Pharmacol.* **2007**, *72*, 197−207. (b) Pedemonte, N.; Sonawane, N. D.; Taddei, A.; Hu, J.; Zegarra-Moran, O.; Suen, Y. F.; Robins, L. I.; Dicus, C. W.; Willenbring, D.; Nantz, M. H.; Kurth, M. J.; Galietta, L. J.; Verkman, A. S. Phenylglycine and sulfonamide correctors of defective ΔF508 and G551D cystic fibrosis transmembrane conductance regulator chloride-channel gating. *Mol. Pharmacol.* **2005**, *67*, 1797−1807. (c) Yang, H.; Shelat, A. A.; Guy, R. K.; Gopinath, V. S.; Ma, T.; Du, K.; Lukacs, G. L.; Taddei, A.; Folli, C.; Pedemonte, N.; Galietta, L. J.; Verkman, A. S. Nanomolar affinity small molecule correctors of defective ΔF508-CFTR chloride channel gating. *J. Biol. Chem.* **2003**, *278*, 35079−35085. (d) Van Goor, F.; Straley, K. S.; Cao, D.; Gonzalez, J.; Hadida, S.; Hazlewood, A.; Joubran, J.; Knapp, T.; Makings, L. R.; Miller, M.; Neuberger, T.; Olson, E.; Panchenko, V.; Rader, J.; Singh, A.; Stack, J. H.; Tung, R.; Grootenhuis, P. D.; Negulescu, P. Rescue of DeltaF508-CFTR trafficking and gating in human cystic fibrosis airway primary cultures by small molecules. *Am. J. Physiol.: Lung Cell. Mol. Physiol.* **2006**, *290*, L1117−L1130. (e) Van Goor, F.; Hadida, S.; Grootenhuis, P. D.; Burton, B.; Cao, D.; Neuberger, T.; Turnbull, A.; Singh, A.; Joubran, J.; Hazlewood, A.; Zhou, J.; McCartney, I.; Arumugam, V.; Decker, C.; Yang, J.; Young, C.; Olson, E. R.; Wine, J. J.; Frizzell, R. A.; Ashlock, M.; Negulescu, P. Rescue of CF airway epithelial cell function in vitro by a CFTR potentiator, VX-770. *Proc. Natl Acad. Sci. U.S.A.* **2009**, *106*, 18825−18830. (f) Accurso, F. J.; Rowe, S. M.; Clancy, J. P.; Boyle, M. P.; Dunitz, J. M.; Durie, P. R.; Sagel, S. D.; Hornick, D. B.; Konstan, M. W.; Donaldson, S. H.; Moss, R. B.; Pilewski, J. M.; Rubenstein, R. C.; Uluer, A. Z.; Aitken, M. L.; Freedman, S. D.; Rose, L. M.; Mayer-Hamblett, N.; Dong, Q.; Zha, J.; Stone, A. J.; Olson, E. R.; Ordonez, C. L.; Campbell, P. W.; Ashlock, M. A.; Ramsey, B. W. Effect of VX-770 in persons with cystic fibrosis and the G551D-CFTR mutation. *N. Engl. J. Med.* **2010**, *363*, 1991−2003. (g) Mills, A. D.; Yoo, C.; Butler, J. D.; Yang, B.; Verkman, A. S.; Kurth, M. J. Design and synthesis of a hybrid potentiator−corrector agonist of the cystic fibrosis mutant protein DeltaF508-CFTR. *Bioorg. Med. Chem. Lett.* **2010**, *20*, 87−91. (h) Jones, A. M.; Helm, J. M. Emerging treatments in cystic fibrosis. *Drugs* **2009**, *69*, 1903−1910.

(8) Phuan, P.-W.; Yang, B.; Knapp, J. M.; Wood, A. B.; Lukacs, G. L.; Kurth, M. J.; Verkman, A. S. Cyanoquinolines with independent corrector and potentiator activities restore ΔF508-CFTR chloride channel function in cystic fibrosis. *Mol. Pharmacol.* **2011**, *80*, 683−693.

(9) Solomon, V. R.; Lee, H. Quinoline as a privileged scaffold in cancer drug discovery. *Curr. Med. Chem.* **2011**, *18*, 1488−508.

(10) Massarani, E.; Nardi, D.; Pozzi, R.; Degen, L.; Magistretti, M. J. 8-Hydroxyquinoline derivatives. Synthesis and biological evaluation of arylglyoxal *N*-7-amino-5-substituted 8-hydroxyquinoline hemiacetals and 5-phenylglyoxylidenamino-8-hydroxyquinolines. *J. Med. Chem.* **1970**, *13*, 380−383.

(11) Heiniger, B.; Gakhar, G.; Prasain, K.; Hua, D. H.; Nguyen, T. A. Second-generation substituted quinolines as anticancer drugs for breast cancer. *Anticancer Res.* **2010**, *30*, 3927−3932.

(12) (a) Fischer, O.; Muller, A.; Vilsmeier, A. Action of phosphorus oxychloride upon methyl- and ethylacetanilide. Synthesis of γ-chloroisoquinocyanines. *J. Prakt. Chem.* **1925**, *109*, 69−87. (b) Vilsmeier, A.; Haack, A. Action of phosphorus halides on alkylformanilides. A new method for the preparation of secondary and tertiary *p*-alkylaminonobenzaldehydes. *Ber.* **1927**, *60B*, 119−122. (c) Moussaoui, F.; Belfaitah, A.; Debache, A.; Rhouati, S. Synthesis and characterization of some new aryl quinolyl α,β-unsaturated ketones. *J. Soc. Alger. Chim.* **2002**, *12*, 71−78.

(13) *Spartan '10*; Wavefunction, Inc.: Irvine, CA.

(14) Halgren, T. A. Merck molecular force field. I. Basis, form, scope, parameterization, and performance of MMFF94. *J. Comput. Chem.* **1996**, *17*, 490−519.

(15) Zhao, Y.; Truhlar, D. G. The M06 suite of density functionals for main group thermochemistry, thermochemical kinetics, non-covalent interactions, excited states, and transition elements: two new functionals and systematic testing of four M06-class functionals and 12 other functionals. *Theor. Chem. Acc.* **2008**, *120*, 215−241.

(16) Frisch, M. J.; Trucks, G. W.; Schlegel, H. B.; Scuseria, G. E.; Robb, M. A.; Cheeseman, J. R.; Scalmani, G.; Barone, V.; Mennucci, B.; Petersson, G. A.; Nakatsuji, H.; Caricato, M.; Li, X.; Hratchian, H. P.; Izmaylov, A. F.; Bloino, J.; Zheng, G.; Sonnenberg, J. L.; Hada, M.; Ehara, M.; Toyota, K.; Fukuda, R.; Hasegawa, J.; Ishida, M.; Nakajima, T.; Honda, Y.; Kitao, O.; Nakai, H.; Vreven, T.; Montgomery, J. A., Jr.; Peralta, J. E.; Ogliaro, F.; Bearpark, M.; Heyd, J. J.; Brothers, E.; Kudin, K. N.; Staroverov, V. N.; Kobayashi, R.; Normand, J.; Raghavachari, K.; Rendell, A.; Burant, J. C.; Iyengar, S. S.; Tomasi, J.; Cossi, M.; Rega, N.; Millam, N. J.; Klene, M.; Knox, J. E.; Cross, J. B.; Bakken, V.; Adamo, C.; Jaramillo, J.; Gomperts, R.; Stratmann, R. E.; Yazyev, O.; Austin, A. J.; Cammi, R.; Pomelli, C.; Ochterski, J. W.; Martin, R. L.; Morokuma, K.; Zakrzewski, V. G.; Voth, G. A.; Salvador, P.; Dannenberg, J. J.; Dapprich, S.; Daniels, A. D.; Farkas, Ö.; Foresman, J. B.; Ortiz, J. V.; Cioslowski, J.; Fox, D. J. *Gaussian 09*, revision B.01; Gaussian, Inc., Wallingford CT, 2009.

(17) Marenich, A. V.; Cramer, C. J.; Truhlar, D. G. Universal solvation model based on solute electron density and a continuum model of the solvent defined by the bulk dielectric constant and atomic surface tensions. *J. Phys. Chem. B* **2009**, *113*, 6378−6396.

(18) Since conformations preferred in water are often substantially different from bioactive conformations, the energy penalties associated with changing between them can contribute significantly to energies of binding.

(19) Chang, Y.-P.; Su, T.-M.; Li, T.-W.; Chao, I. Intramolecular hydrogen bonding, gauche interactions, and thermodynamic functions of 1,2-ethanediamine, 1,2-ethanediol, and 2-aminoethanol: a global conformational analysis. *J. Phys. Chem. A* **1997**, *101*, 6107−6117.